Supporting Information for

Lightweight Multifunctional Interlayer of Sulfur–Nitrogen Dual-Doped Graphene for Ultrafast, Long-life Lithium–Sulfur Batteries

Lu Wang,[a] Zhi Yang*,[a] Huagui Nie,[a] Cancan Gu,[a] Wuxing Hua,[a] Xiangju Xu,[a] Xi'an Chen,[a]Ying Chen,[b] Shaoming Huang*,[a]

[a] *Nanomaterials & Chemistry Key Laboratory, Wenzhou University, Wenzhou, 325027, China. E-mail: yang201079@126.com, smhuang@wzu.edu.cn.*

[b] *Institute for Frontier Materials, Deakin University, Geelong campus at Waurn Ponds, Victoria 3216, Australia.*

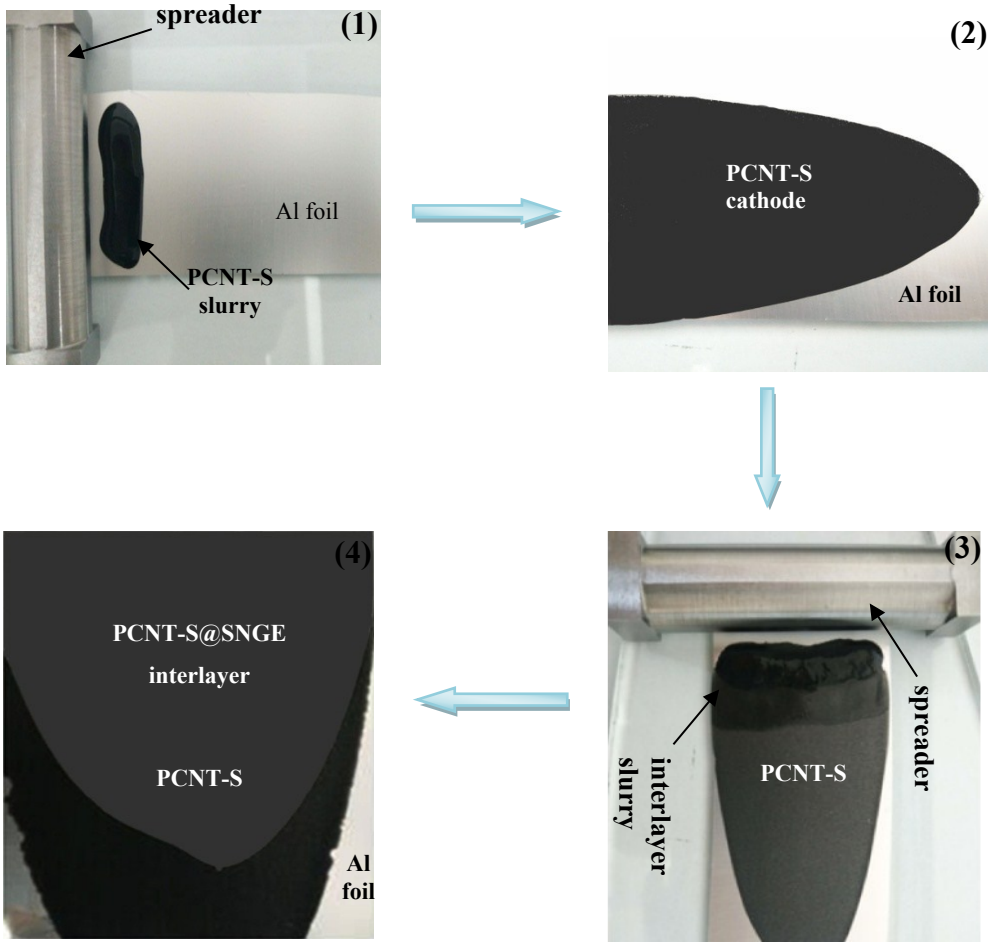

Figure S1 Typical photographs of the coating procedure of PCNT-S cathode (1), (2); cathode coated with SNGE interlayer (3), (4).

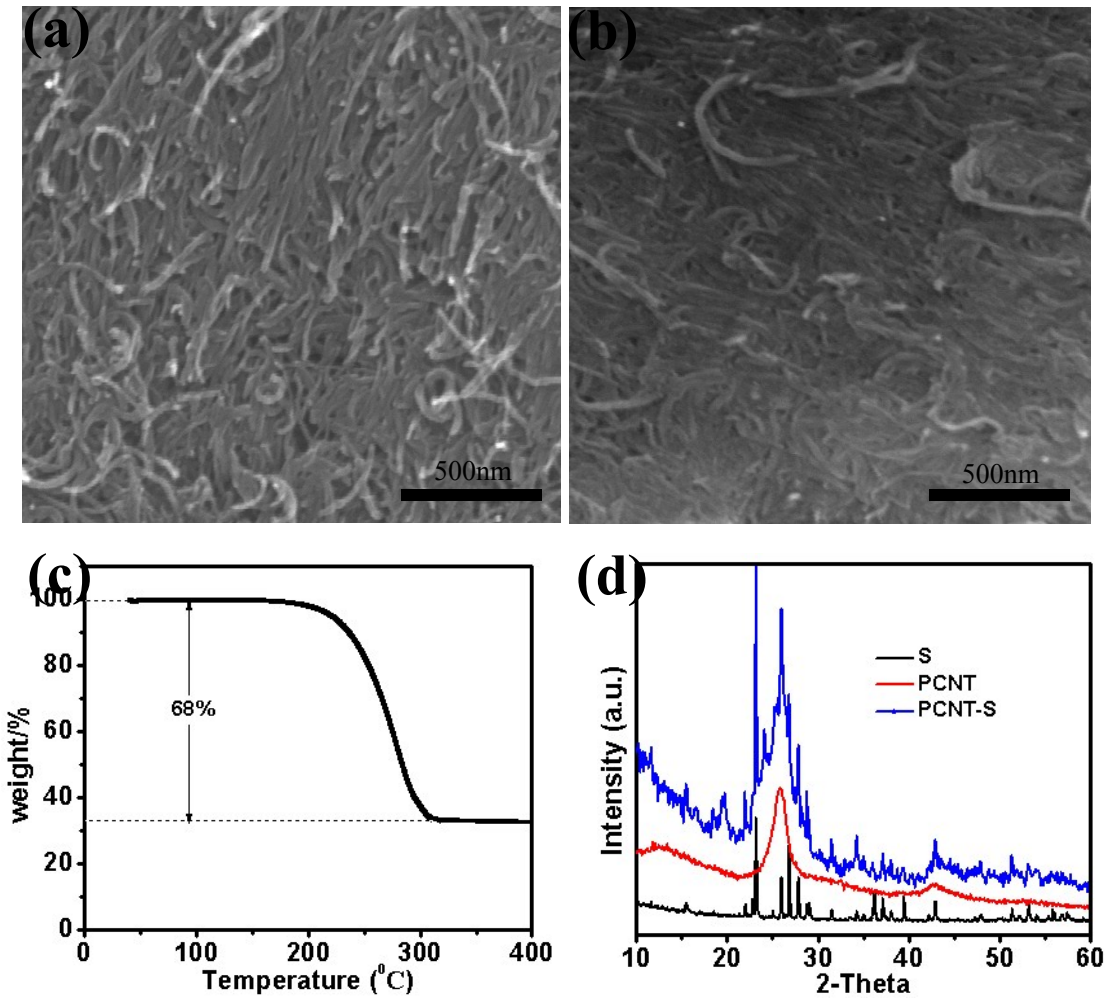

Figure S2 SEM images of PCNT (a) and PCNT-S composite (b); (c) TGA curve of the PCNTs-S composite; (d) XRD patterns of S, PCNT and PCNT-S composite.

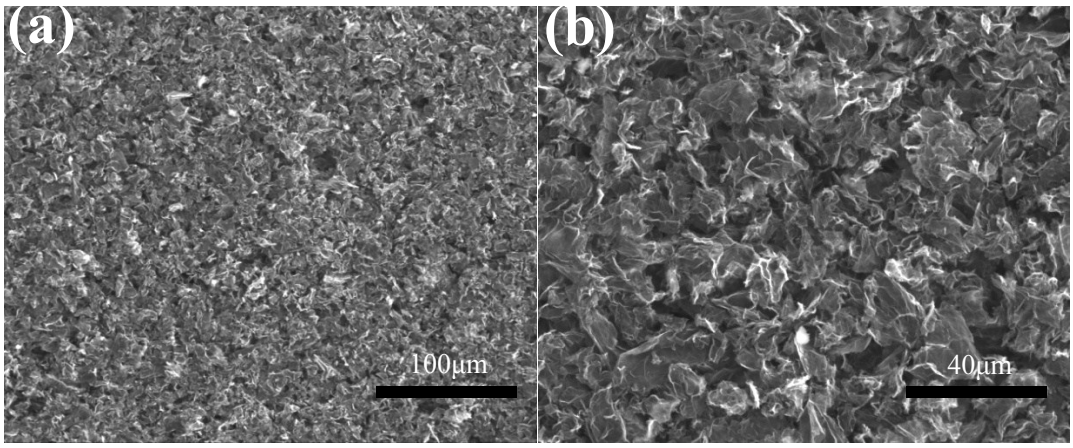

Figure S3 Top-view SEM images of fresh PCNT-S@SNGE cathode at different resolution.

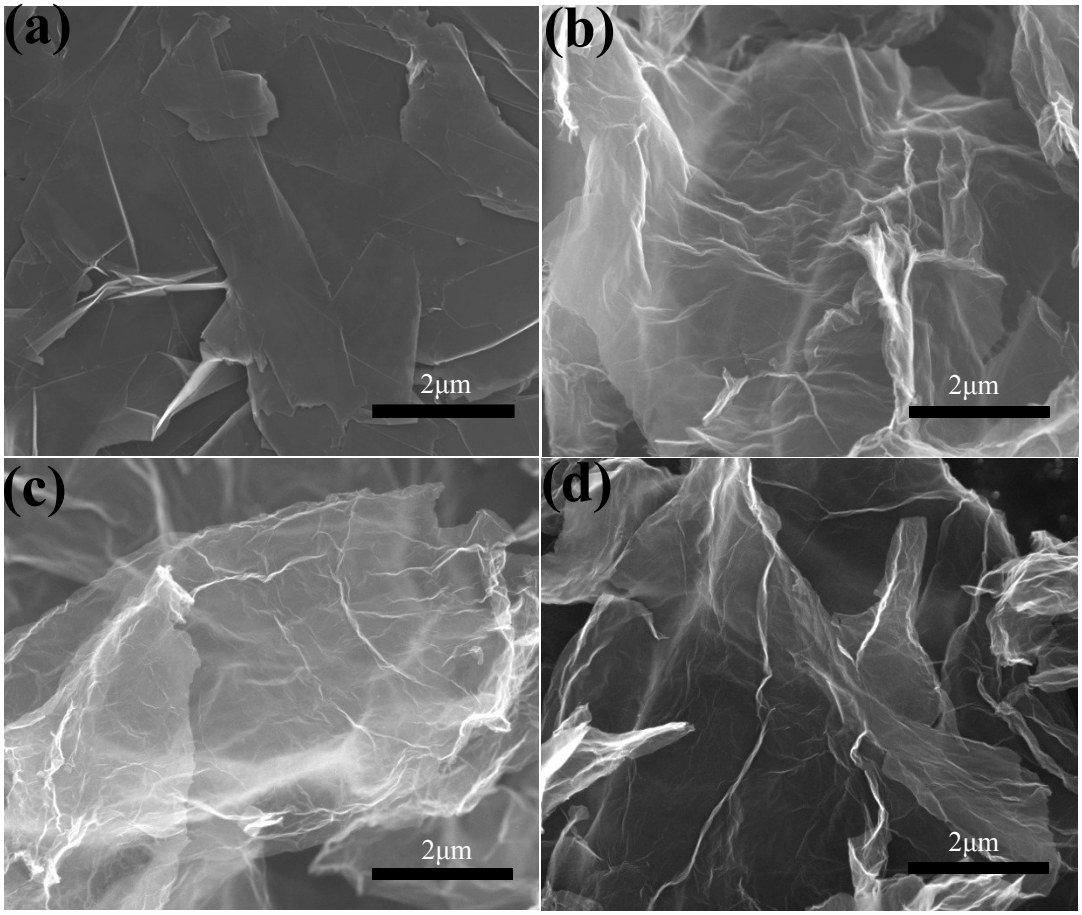

Figure S4 SEM images of rGO (a), SGE (b), NGE (c) and SNGE (d).

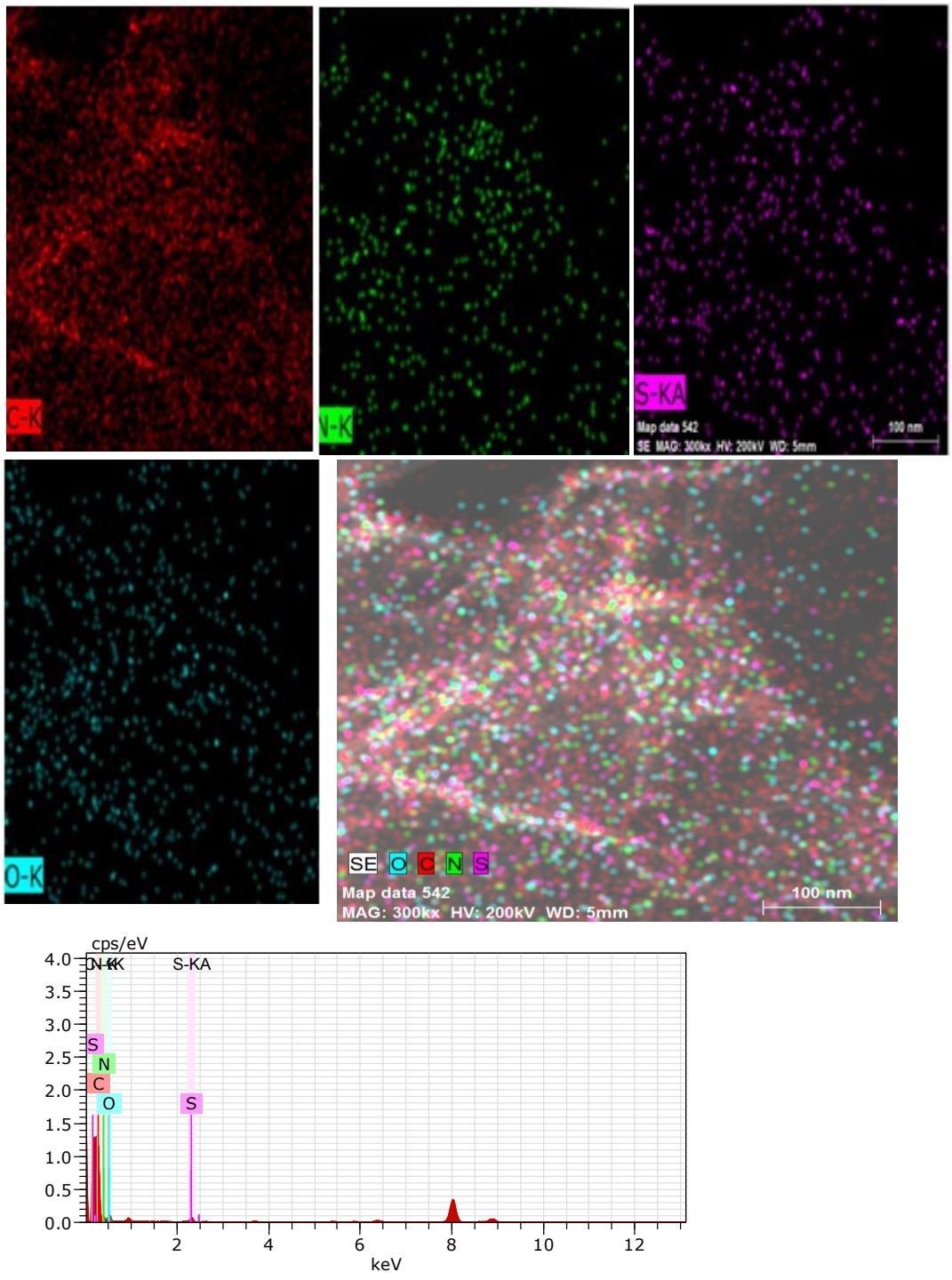

Figure S5 TEM maping and EDX of SNGE.

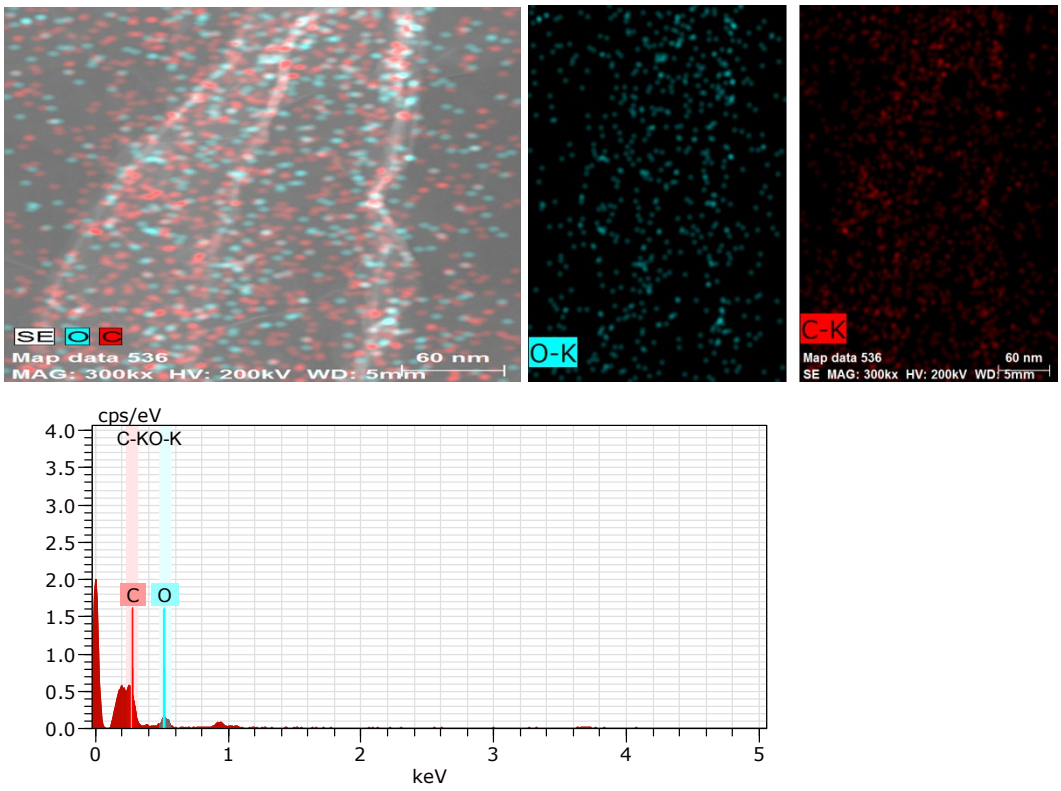

Figure S6 TEM maping and EDX of rGO.

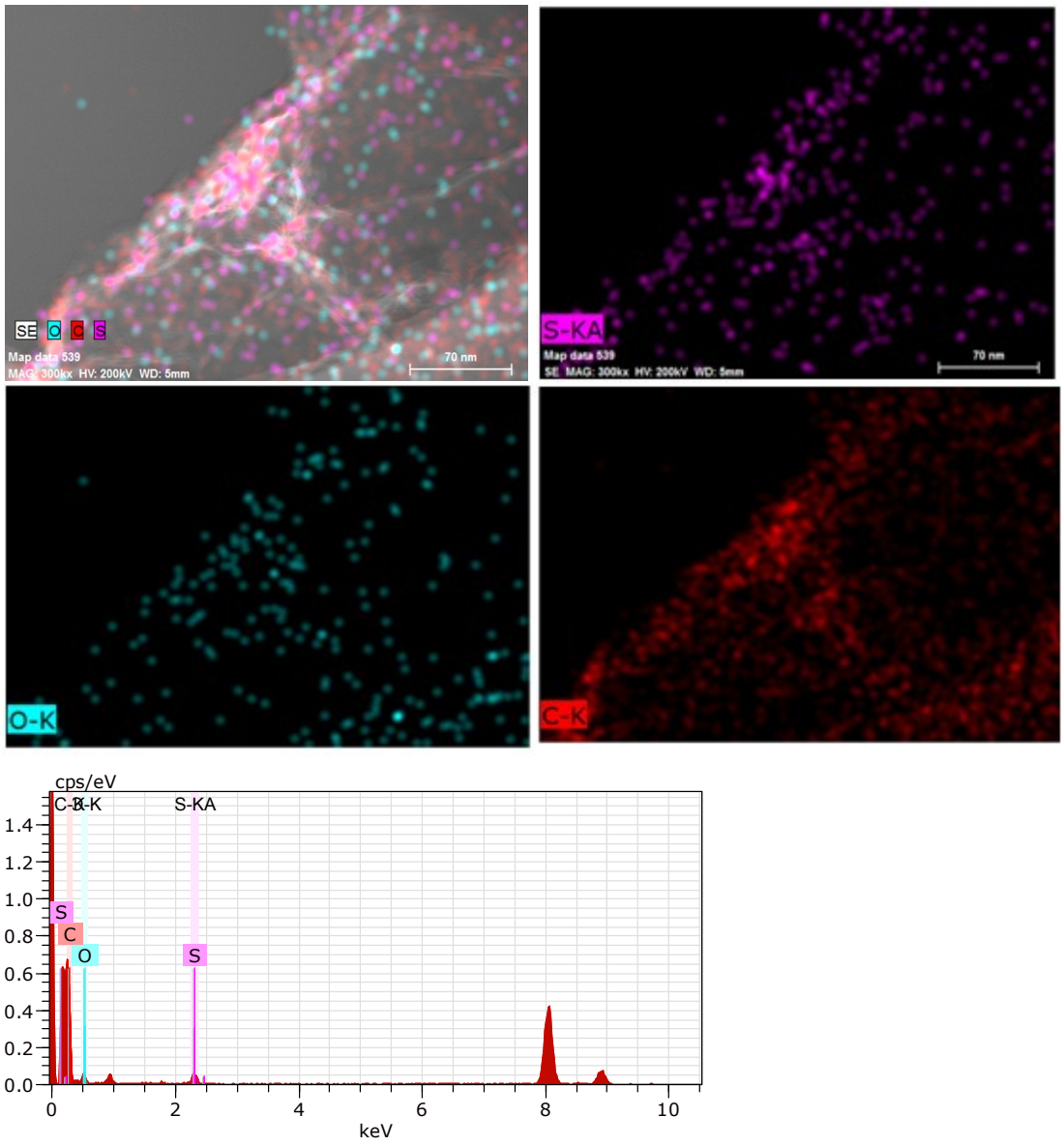

Figure S7 TEM maping and EDX of SGE.

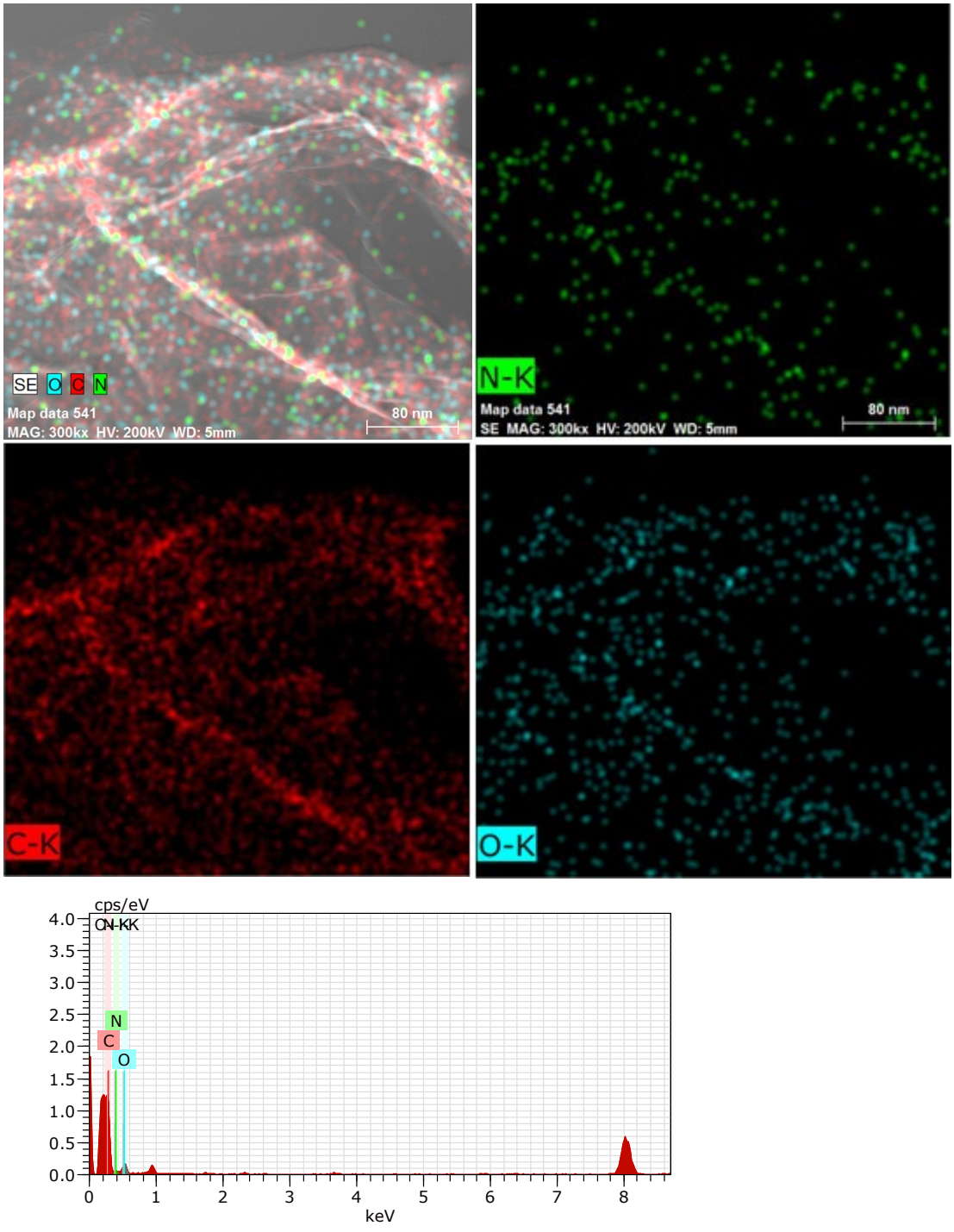

Figure S8 TEM maping and EDX of NGE.

Table S1 Elemental contents of for rGO, SGE, NGE, and SNGE

Sample	C(at%)	O(at%)	N(at%)	S(at%)
rGO	97.04	2.96	—	—
SGE	93.72	3.34	—	2.94
NGE	95.28	2.5	2.22	—
SNGE	80.87	11.97	6.01	1.15

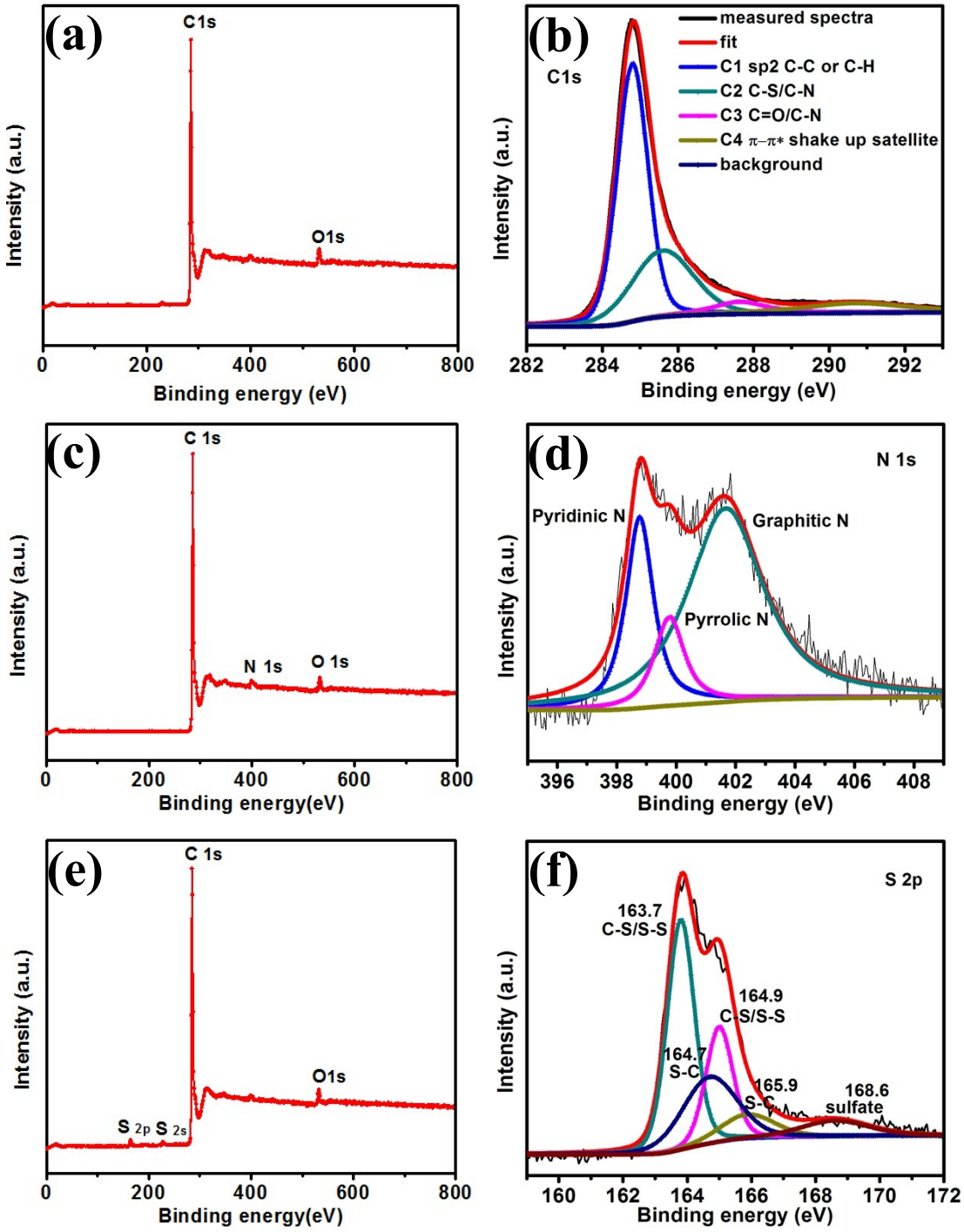

Figure S9 XPS survey (a) of rGO; high-resolution C1s of SNGE (b); XPS survey (c) and high-resolution N 2s (d) of NGE; XPS survey (e) and high-resolution S 2p (f) of SGE.

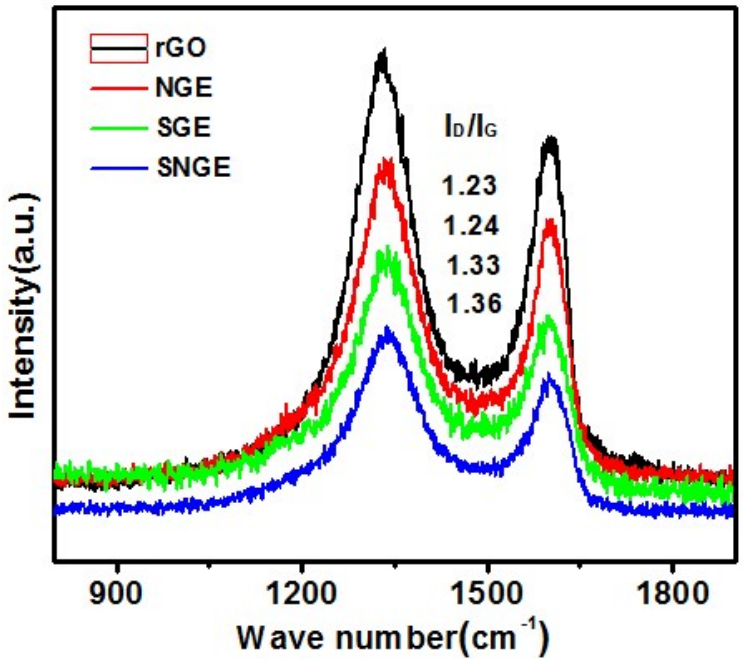

Figure S10 Raman spectra of the four graphene materials.

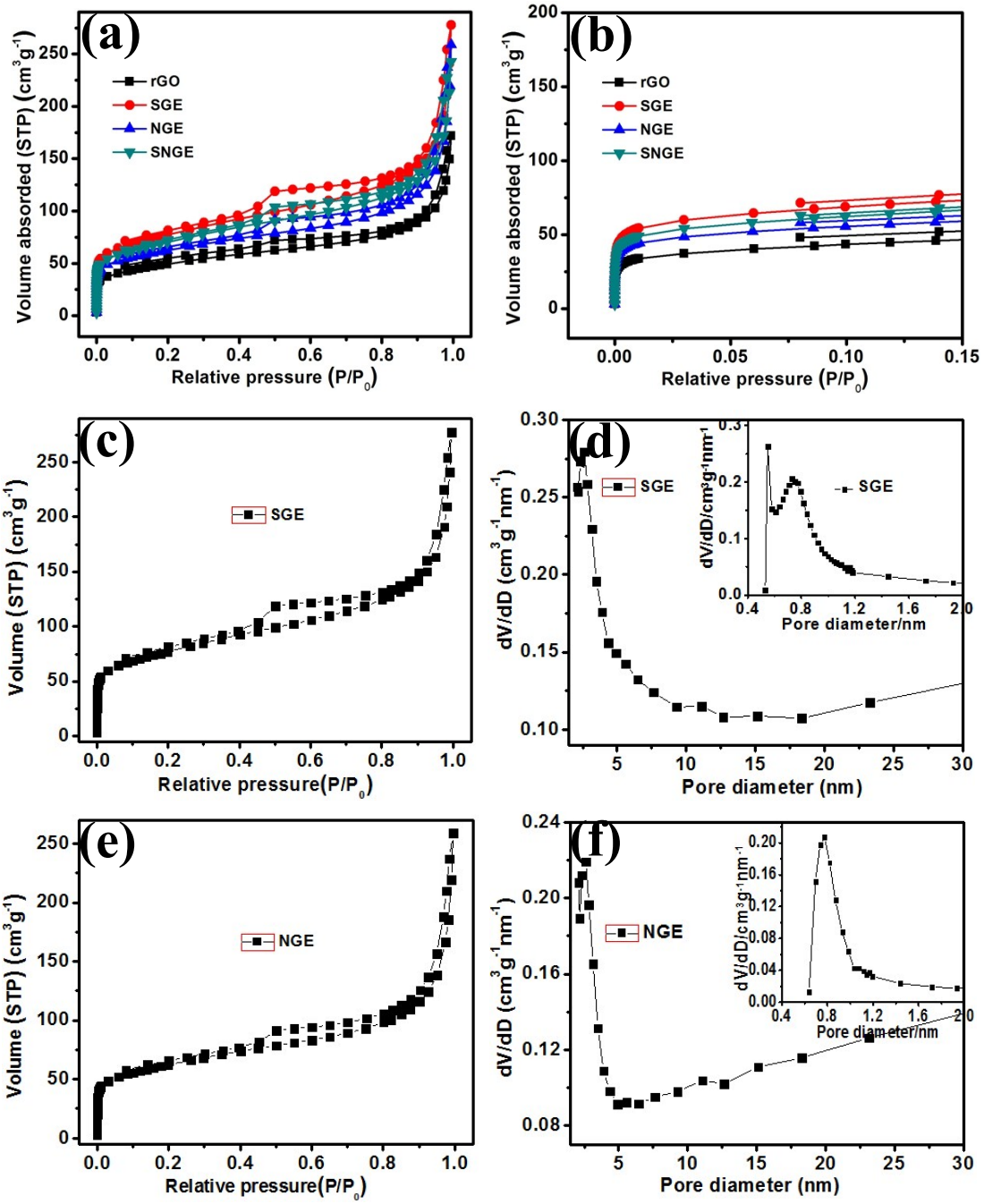

Figure S11 (a),(b) N_2 adsorption/desorption isotherms for the four graphene materials at selected P/P_0 range; N_2 adsorption/desorption isotherm (c) and pore size distribution (d) of SGE; N_2 adsorption/desorption isotherm (e) and pore size distribution (f) of NGE.

Table S2. The surface area and pore volume of rGO, SGE, NGE, SNGE

Sample	BET surface area (m^2/g)	Micropore surface area (m^2/g)	Total pore volume (cm^3/g)	Micropore volume (cm^3/g)	Median width of micropore (nm)
rGO	167.46	69.74	0.27	0.067	0.8030
SGE	261.03	132.58	0.43	0.106	0.7954
NGE	209.87	102.61	0.40	0.086	0.7899
SNGE	239.11	123.01	0.38	0.096	0.7896

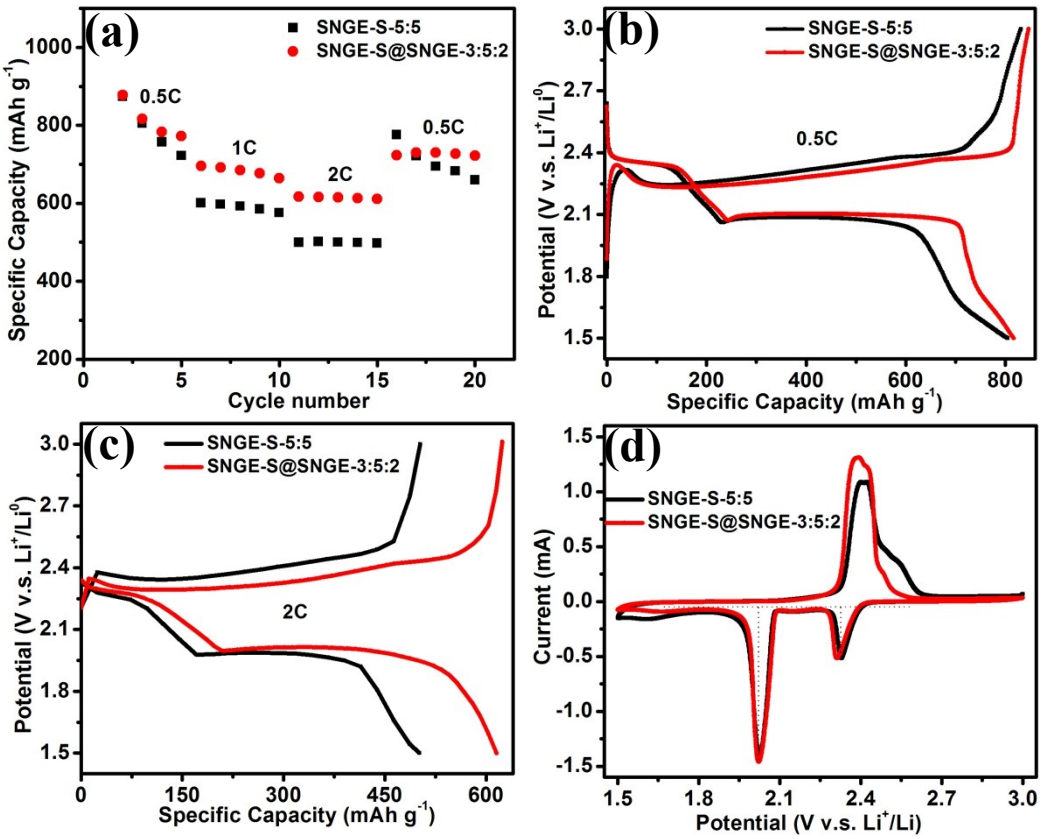

Figure S12 (a) rate performance at various current density; (b) corresponding galvanostatic discharge-charge profiles at 0.5C; (c) galvanostatic discharge-charge profiles at 2C (d) for the two SNGE-S cathodes; (d) CV plots for the two SNGE-S cathode at scan rate of 0.1 mV/s, the areal sulfur loading of the cathodes here are 0.54 mg cm^{-2}.

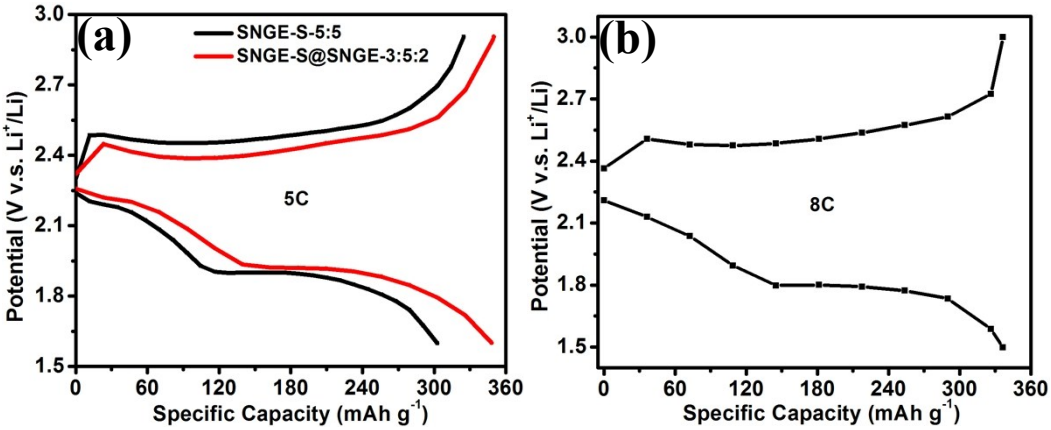

Figure S13 (a) galvanostatic charge/discharge profiles for SNGE-S-5:5 and SNGE-S@SNGE-3:5:2 cathodes; (b) galvanostatic charge/discharge profile for SNGE-S@SNGE-3:5:2 cathode at 8C. The areal sulfur loading of cathodes here were determined to be 0.54 mg cm^{-2}.

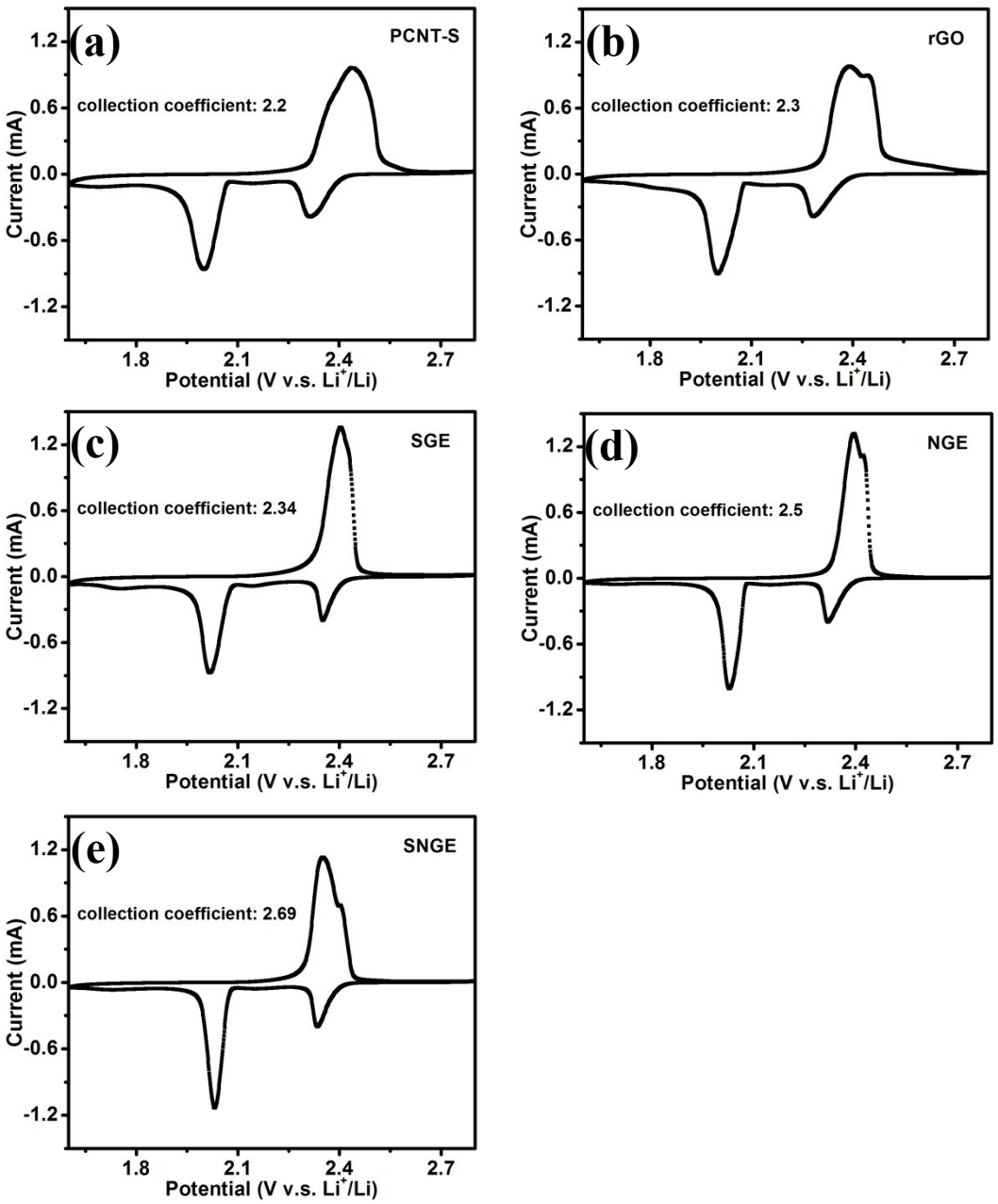

Figure S14 The second CV curves of the five cathodes and their corresponding collection coeffient.

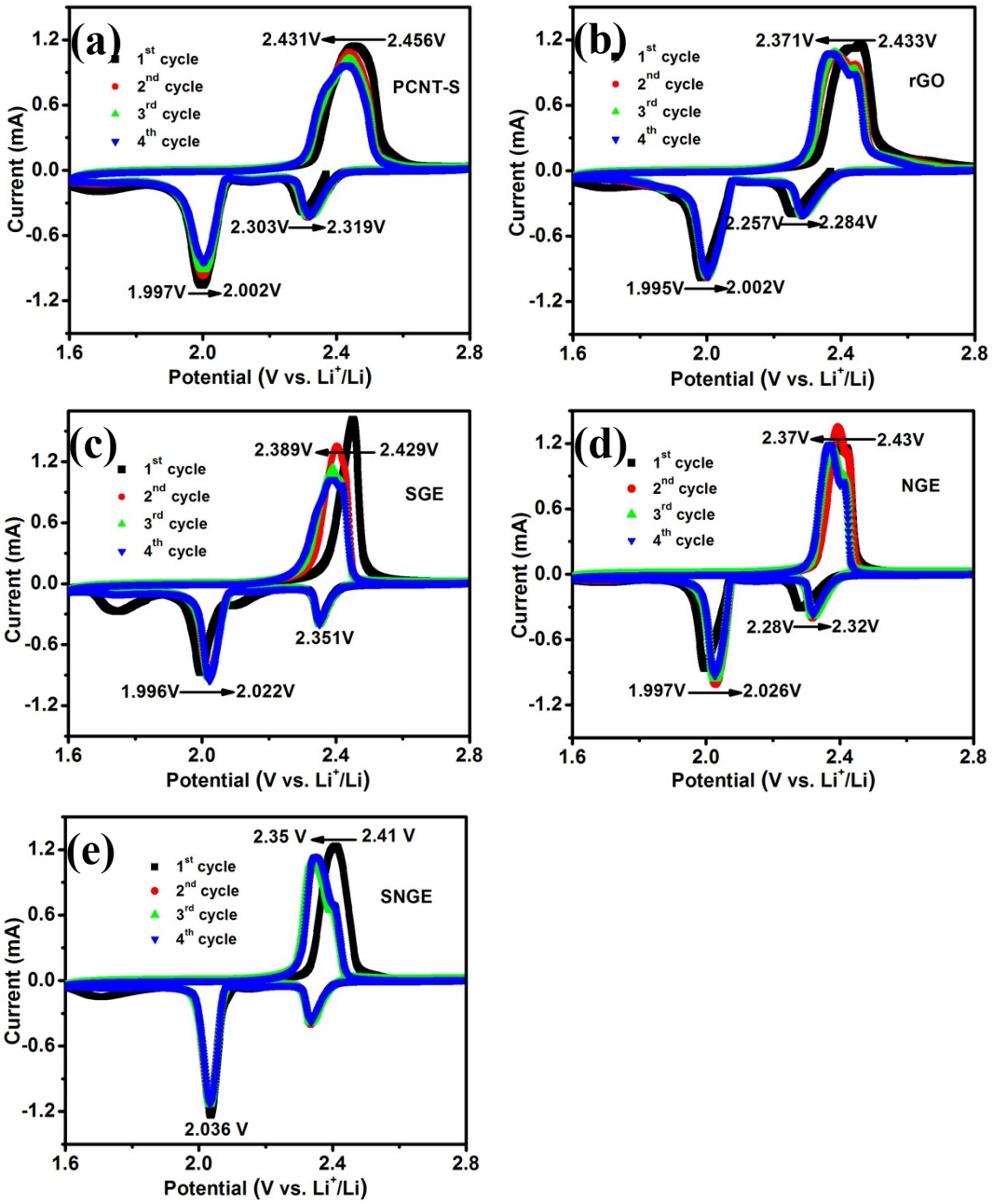

Figure S15 CV curves of the first four cycles for cathode of PCNT-S (a), PCNT-S@rGO (b), PCNT-S@SGE (c), PCNT-S@NGE (d), PCNT-S@SNGE (e).

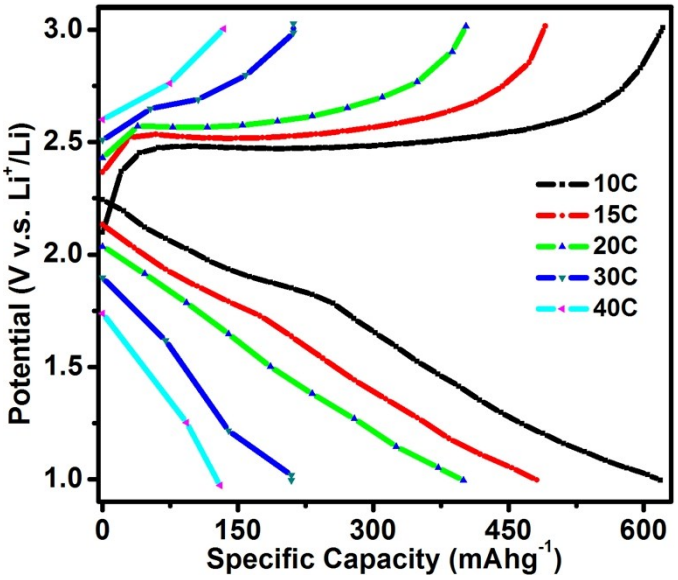

Figure S16 Galvanostatic charge/discharge profiles from 10C to 40C with cut-off voltage of 1V for PCNT-S@SNGE v.s. Li anode.

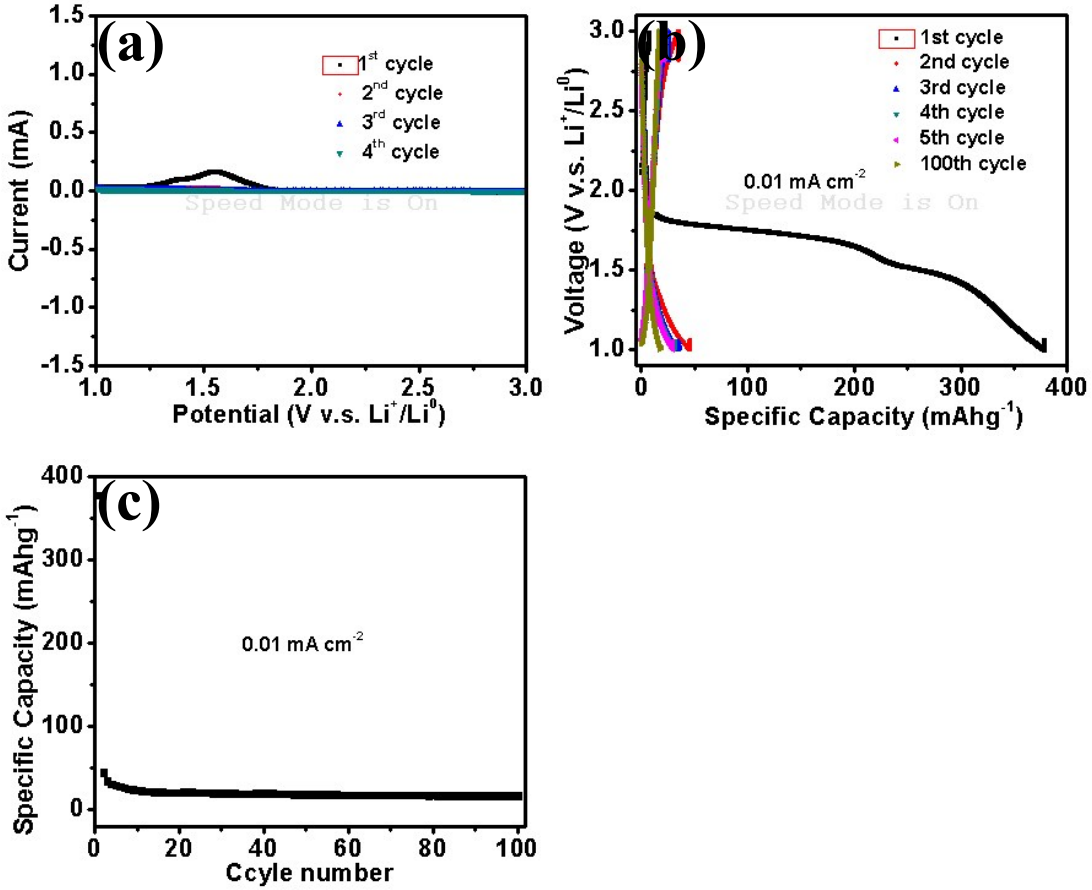

Figure S17 The first four cycles of CV curves (a); galvanostatic charge-discharge profile (b) and cycling performance (c) at a current of 0.01 m Ag^{-1} for the SNGE blank electrode without sulfur loading.

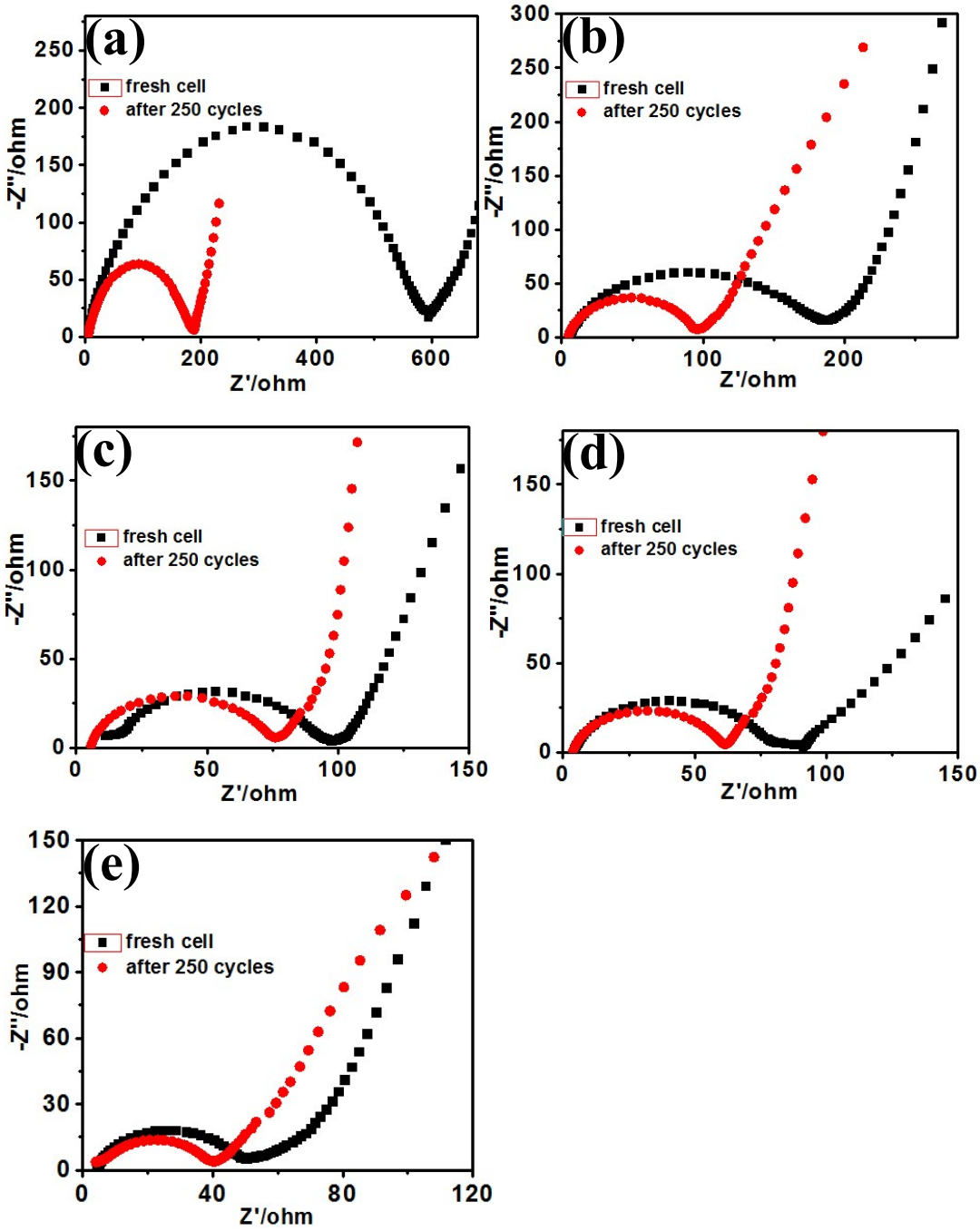

Figure S18 Nyquist plots of cells before cycling and after 250 cycles at rate of 2 C for cathodes of PCNT-S (a), PCNT-S@rGO (b), PCNT-S@SGE (c), PCNT-S@NGE (d), PCNT-S@SNGE (e).

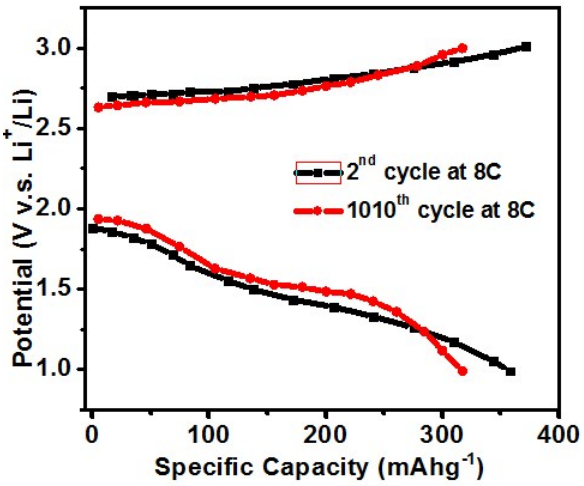

Figure S19 Galvanostatic charge/discharge profiles for the 2nd and 1010th cycles at 8C.

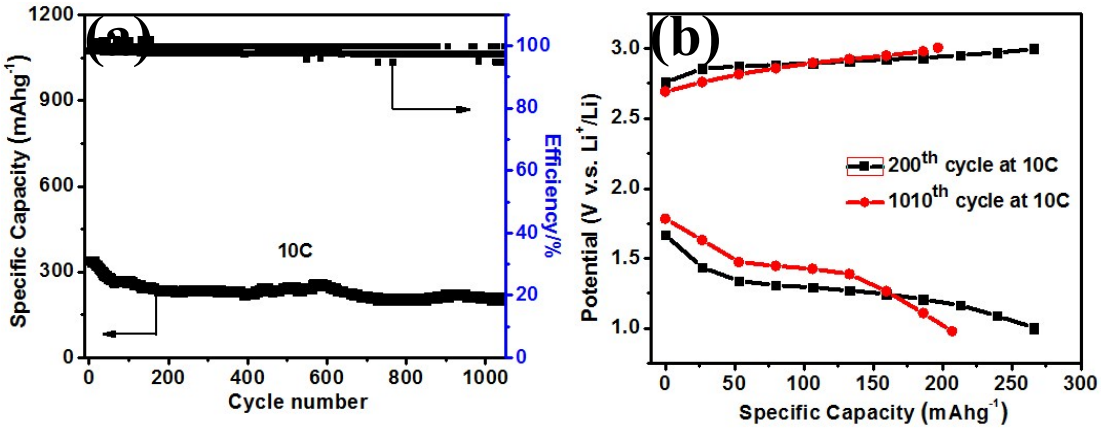

Figure S20 (a) cyclic performance and coulombic efficiency of PCNT-S@SNGE cathode cycled over 1000 cycles at rate of 10 C; (b) the corresponding galvanostatic charge/discharge profiles for the 200th and 1010th cycles at 10 C;

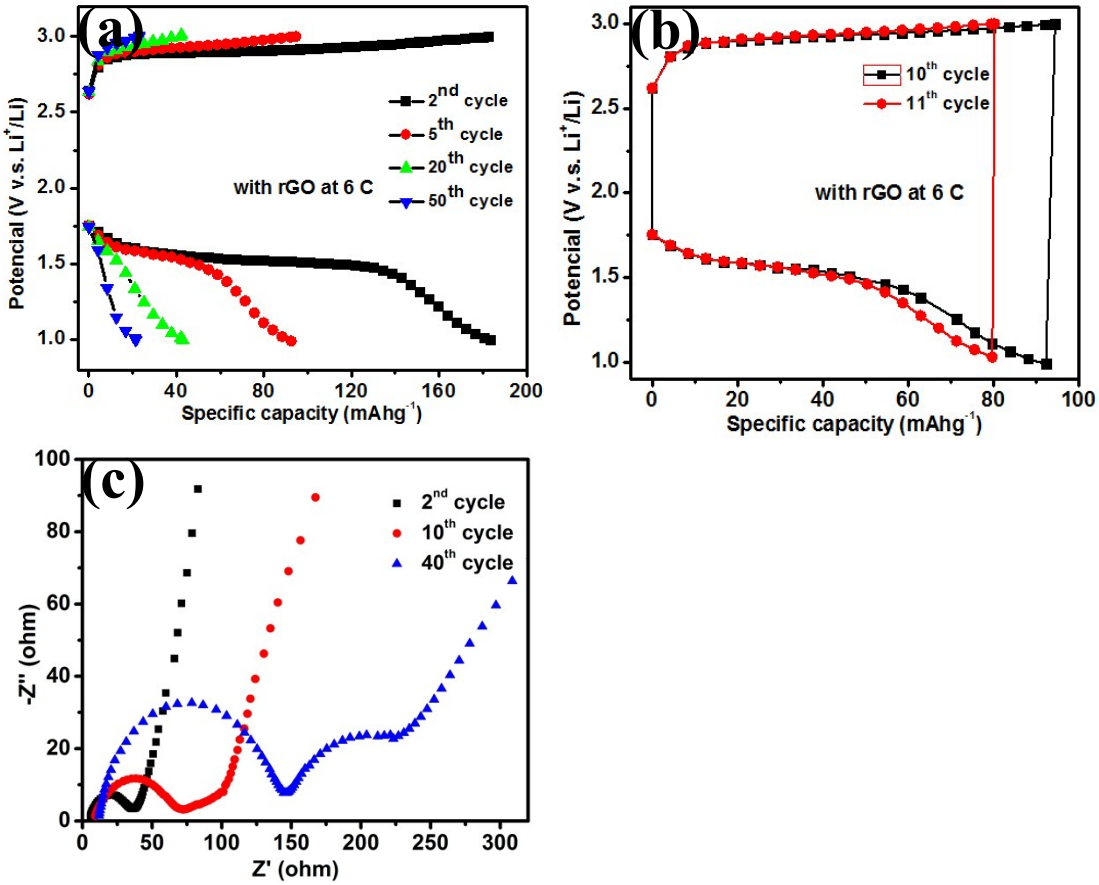

Figure S21 (a) galvanostatic charge/discharge profiles for various cycles at 6 C for PCNT-S@rGO cathode; (b) galvanostatic charge/discharge profiles of 10th and 11th cycles at 6C (difficult in cycling at 8C); (c) Nyquist plots of PCNTs-S@rGO cathode after 50 cycles at 6 C, where the high frequency semicircle is assigned to be associated with charge-transfer resistance (Rct) while the one in the middle frequency region corresponded to the resistance of a passivation film on the electrode, and presence of the latter verified the deposition of Li_2S_2/Li_2S is considered be responsible for the inferior performance of PCNT-S@rGO cathode. [S1]

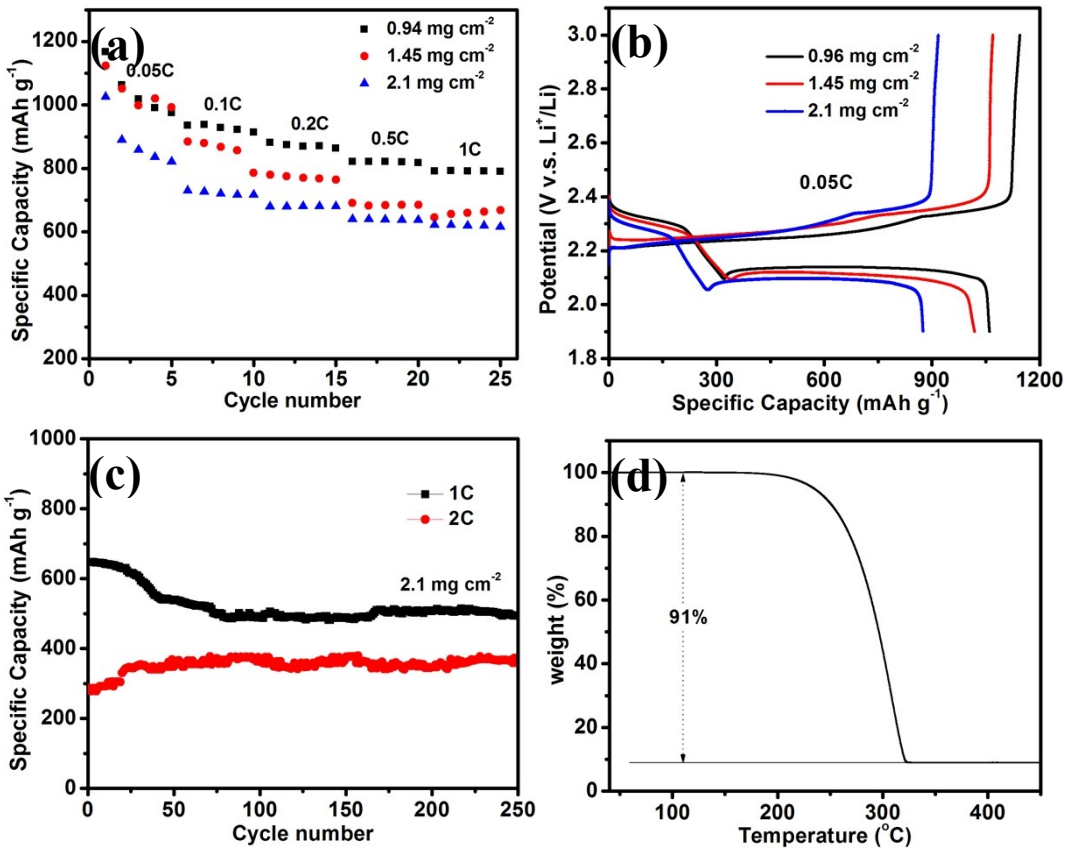

Figure S22 (a) Rate performance of PCNT-S@SNGE cathode with various sulfur areal loading and the corresponding galvanostatic charge-discharge profiles at 0.05C (b); (c) cyclic performance of PCNT-S@SNGE cathode at rate of 1C and 2C;(d) the TGA curve of PCNT-S composite here.

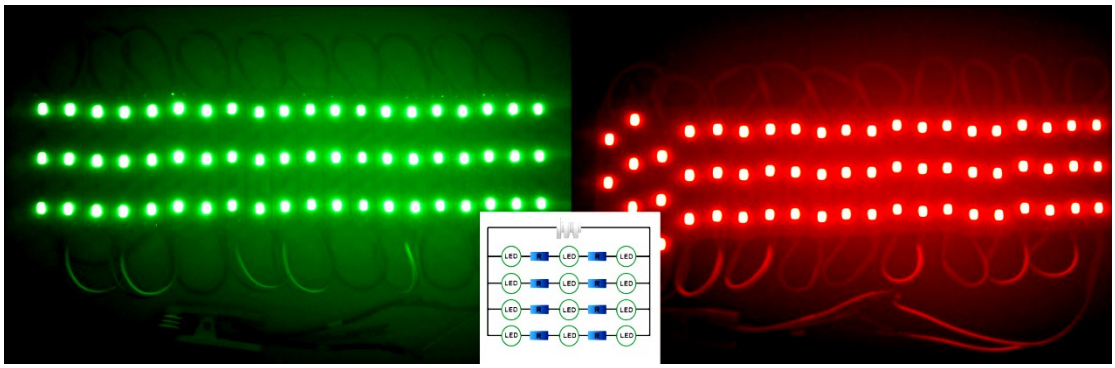

Figure S23 The photographs of our cell for practical application, where three of the cell with 68% sulfur composite cathode could drive 60 green and red indicators of 2835 LED modules (nominal voltage of 12 V and nominal power of 3 W), respectively; inset is the circuit diagram.

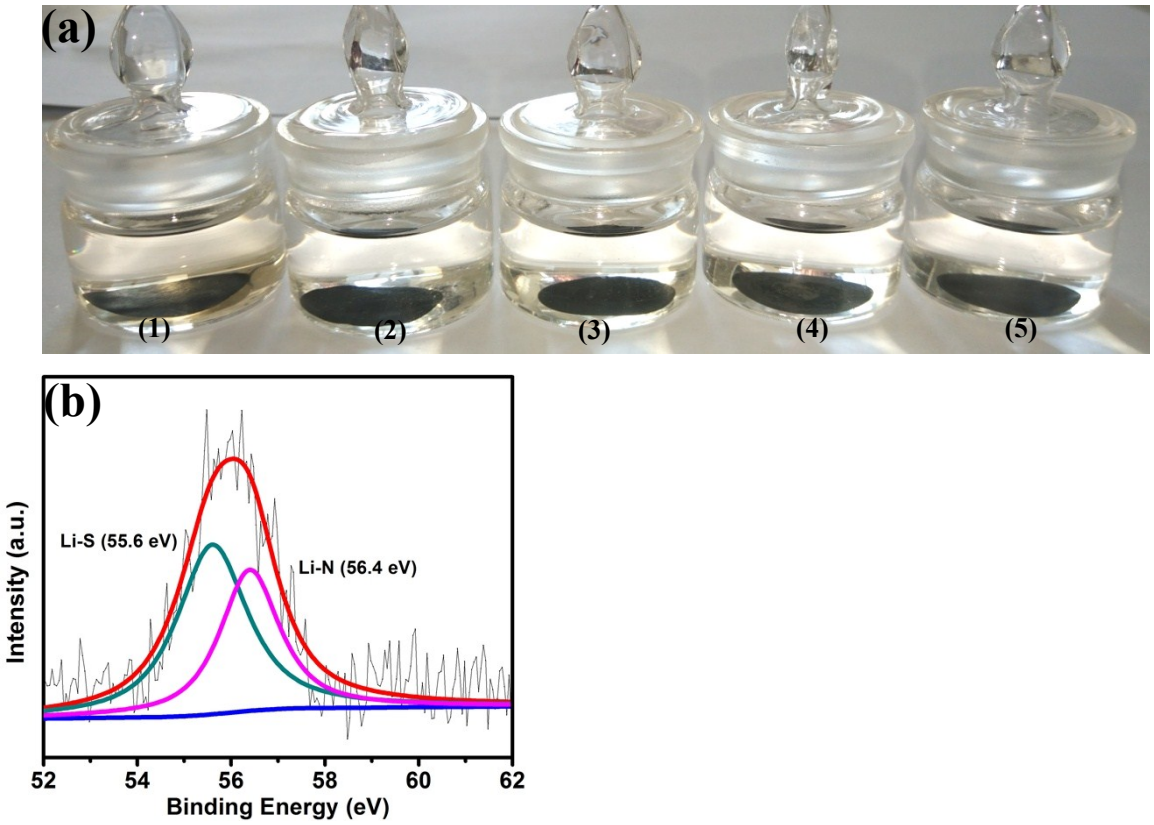

Figure S24 Photographs for (a) the cathodes disassembled from cell at discharged state, (1), (2), (3), (4), (5) corresponding to PCNT-S, PCNT-S@rGO, PCNT-S@SGE, PCNT-S@NGE, PCNT-S@SNGE cathode, respectively; (b) High-resolution XPS spectra of the Li 1s peak for the cycled PCNTs-S@SNGE electrode.

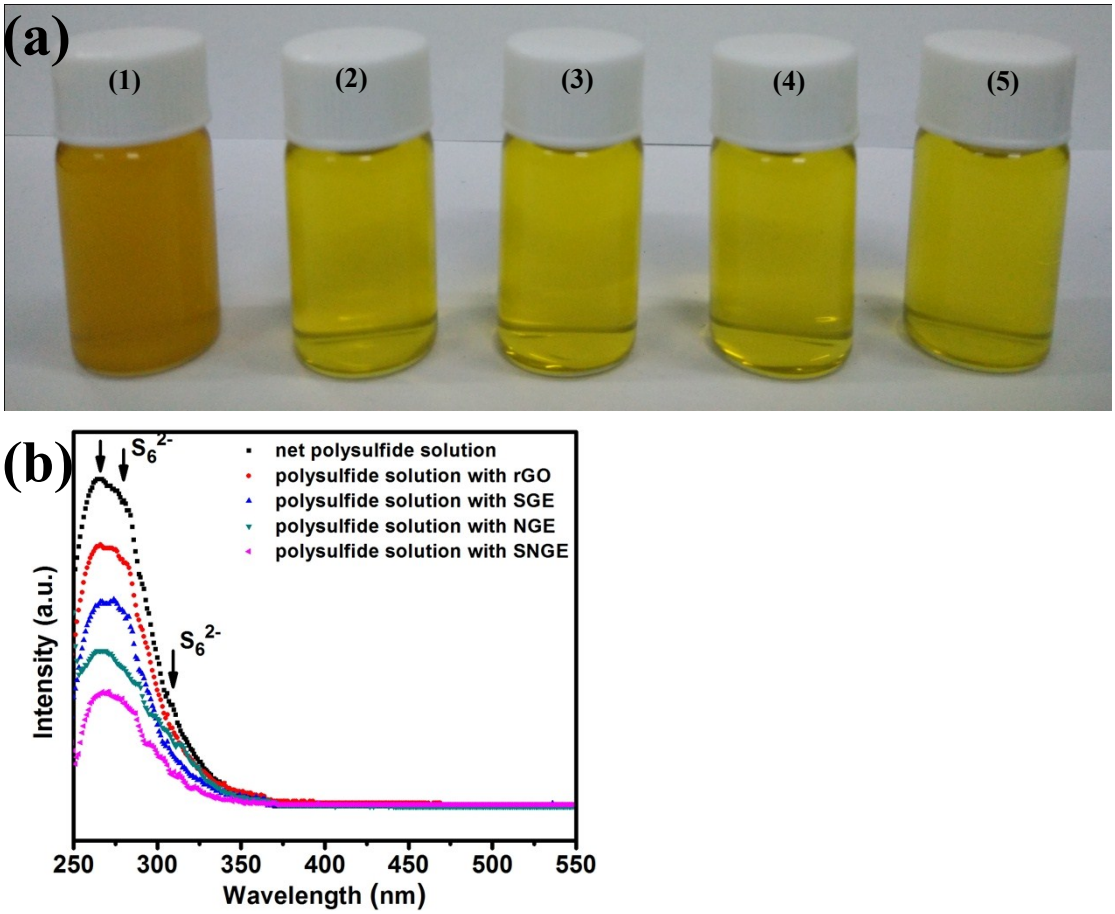

Figure S25 (a) photographs for the original polysulfides solution and polysulfides solution after centrifugal separation of the residue, prior to which the four net graphene materials with same mass were dispersed in polysulfides solution for 12 h absorption, (1), (2), (3), (4), (5) corresponding to original and the ones after absorption of rGO, SGE, NGE, SNGE repectively, and the residues were collected and disperded in alcohol assigned to XPS. (b) UV-vis absorption spectra corresponding to (a). The original polysulfides solution was prepared in electrolyte with short circuit between sulfur cathode and Li anode;

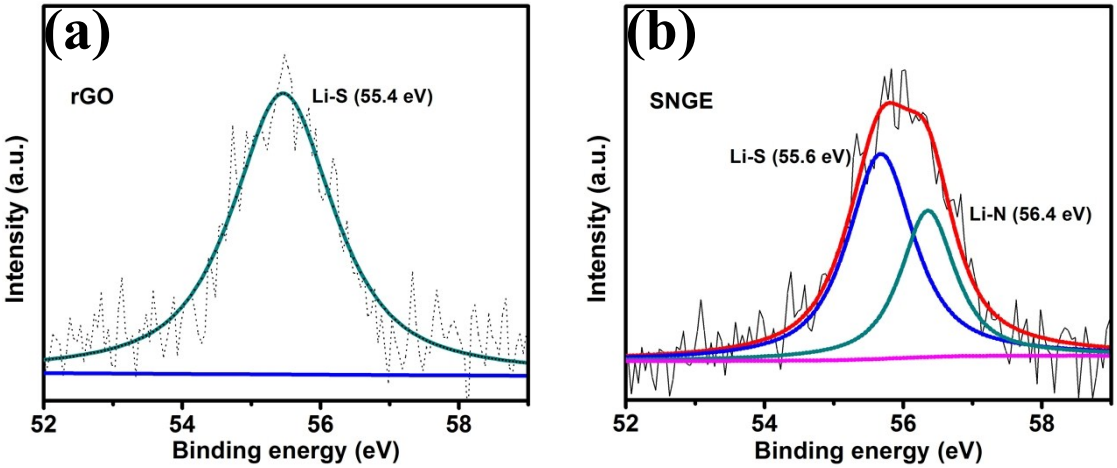

Figure S26 High-resolution XPS spectra of the Li 1s peak of the residues of rGO (a) and SNGE (b) in absorption measurement of the four net interlayer materials.

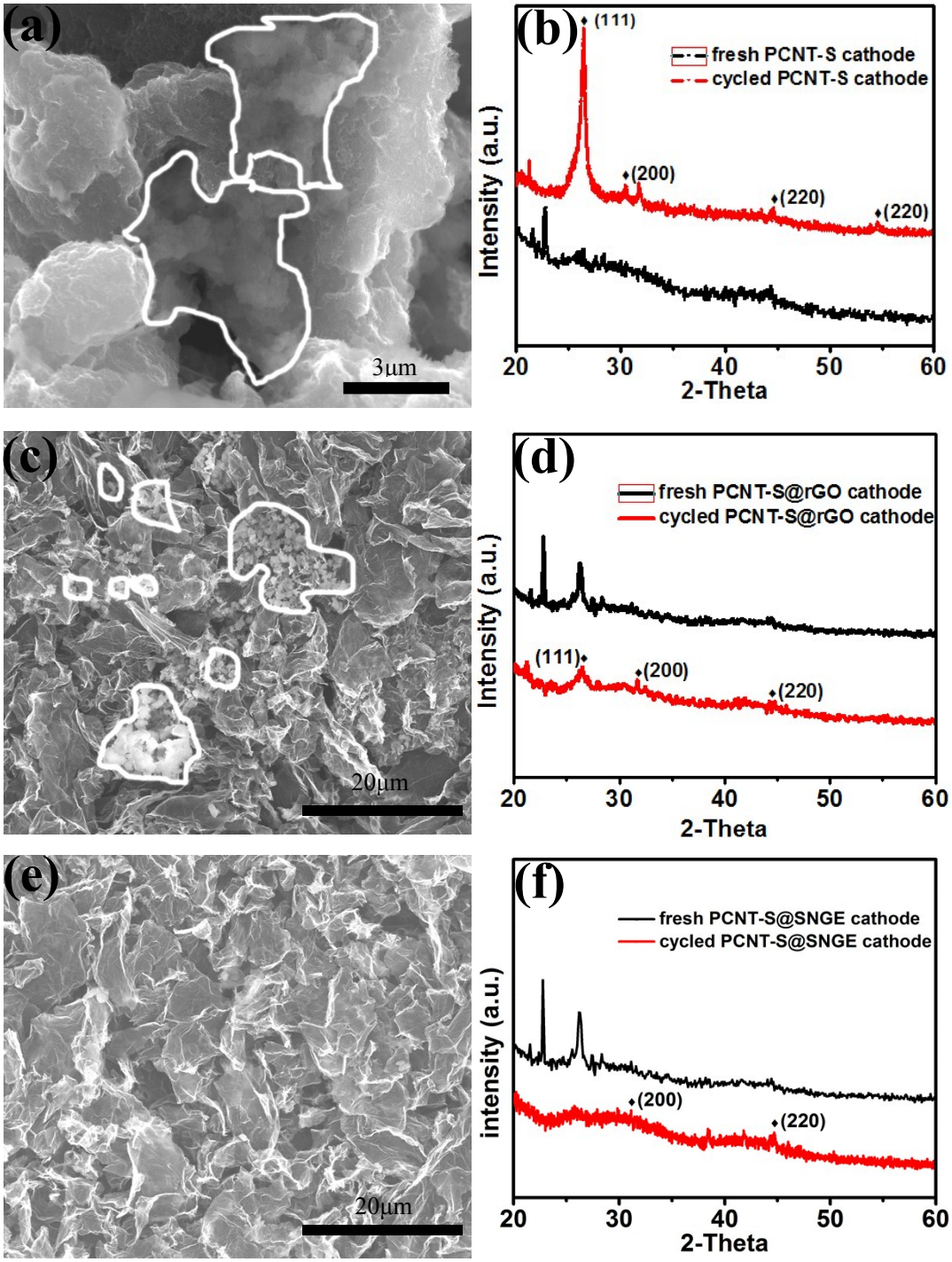

Figure S27 SEM images of cycled cathodes (discharged state) and XRD patterns of Li_2S for the fresh and cycled cathode at 15 C for PCNT-S (a) and (b), PCNT-S@rGO (c) and (d), PCNT-S@SNGE (e) and (f), respectively.

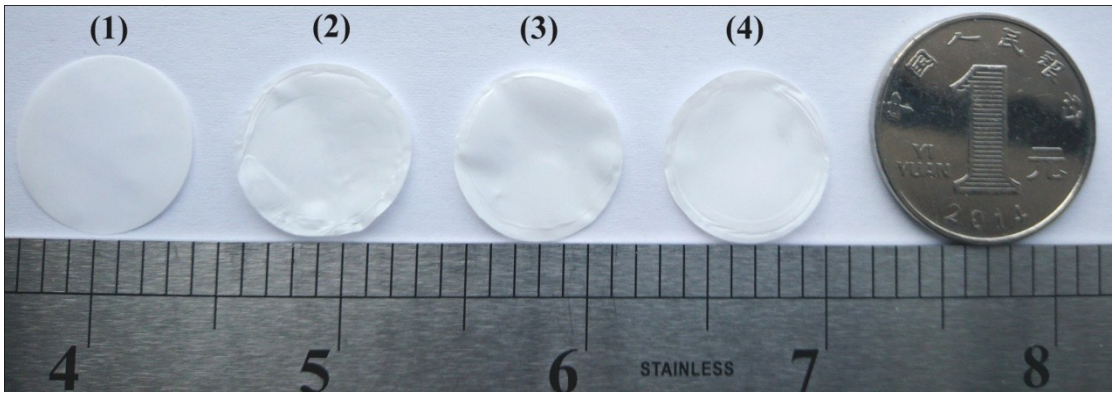

Figure S28 Photographs for the separator of fresh (1), and the ones corresponding to cycled PCNT-S cathode (2), cycled PCNT-S@rGO cathode (3), and cycled PCNT-S@SNGE (4), respectively.

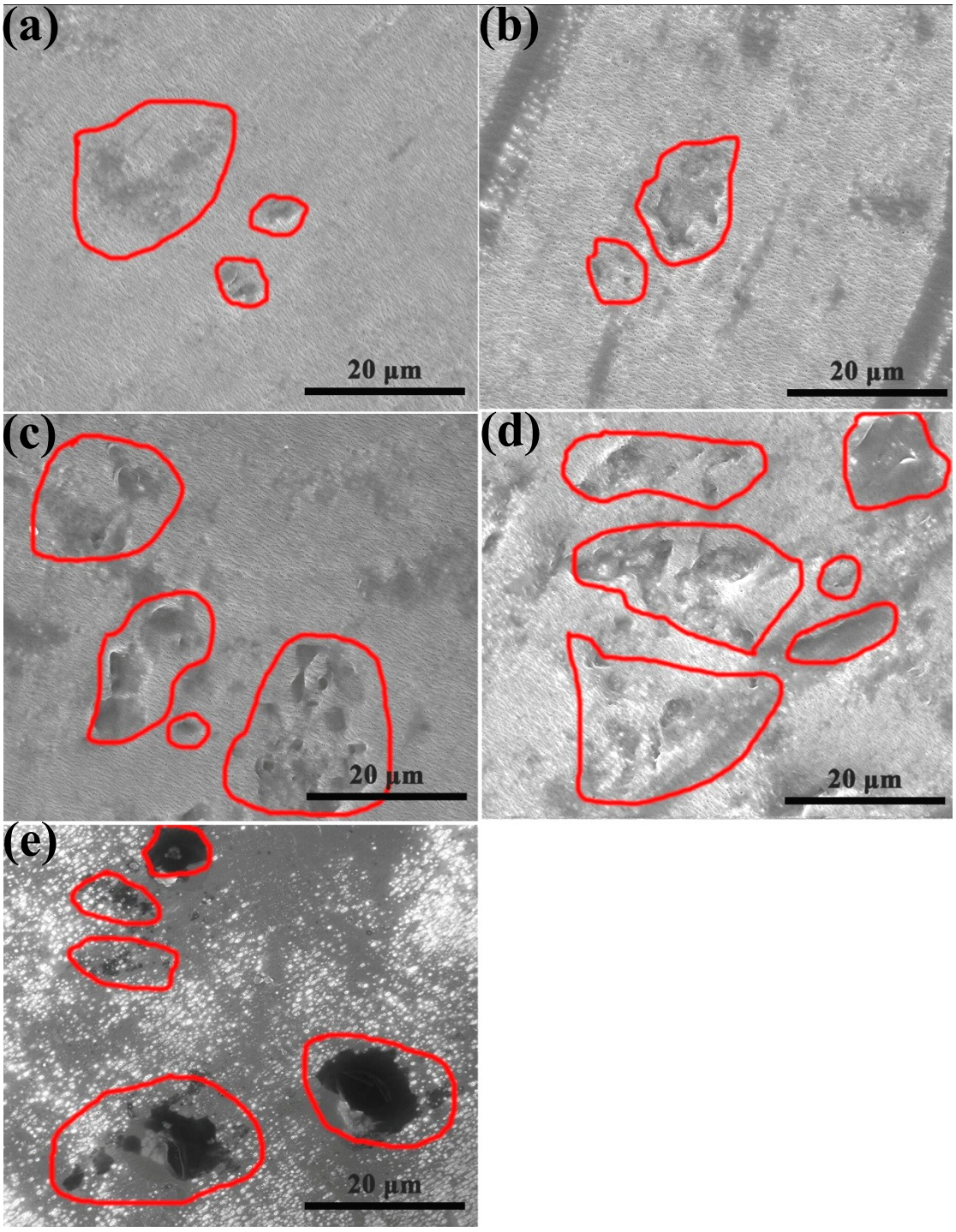

Figure S29 SEM images of the separators matched with PCNT-S electrode cycled at rate of (a) 3 C, (b) 5 C, (c) 10 C, (d) 15 C, (e) 20C, respectively

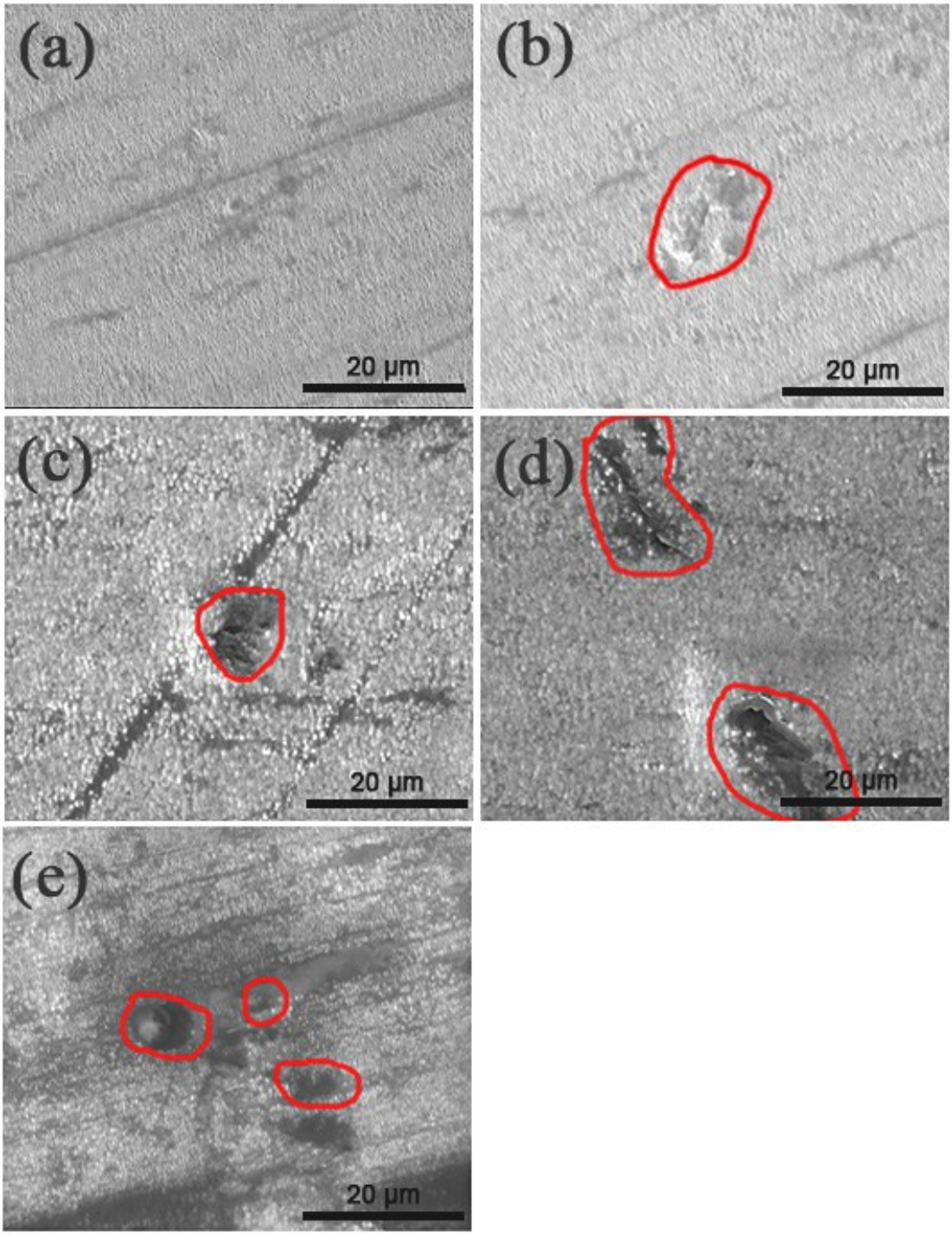

Figure S30 SEM images of the separator matched with PCNT-S@GE electrode cycled at rate of (a) 3C, (b) 5C, (c) 10C, (d) 15C, (e) 30 C, respectively.

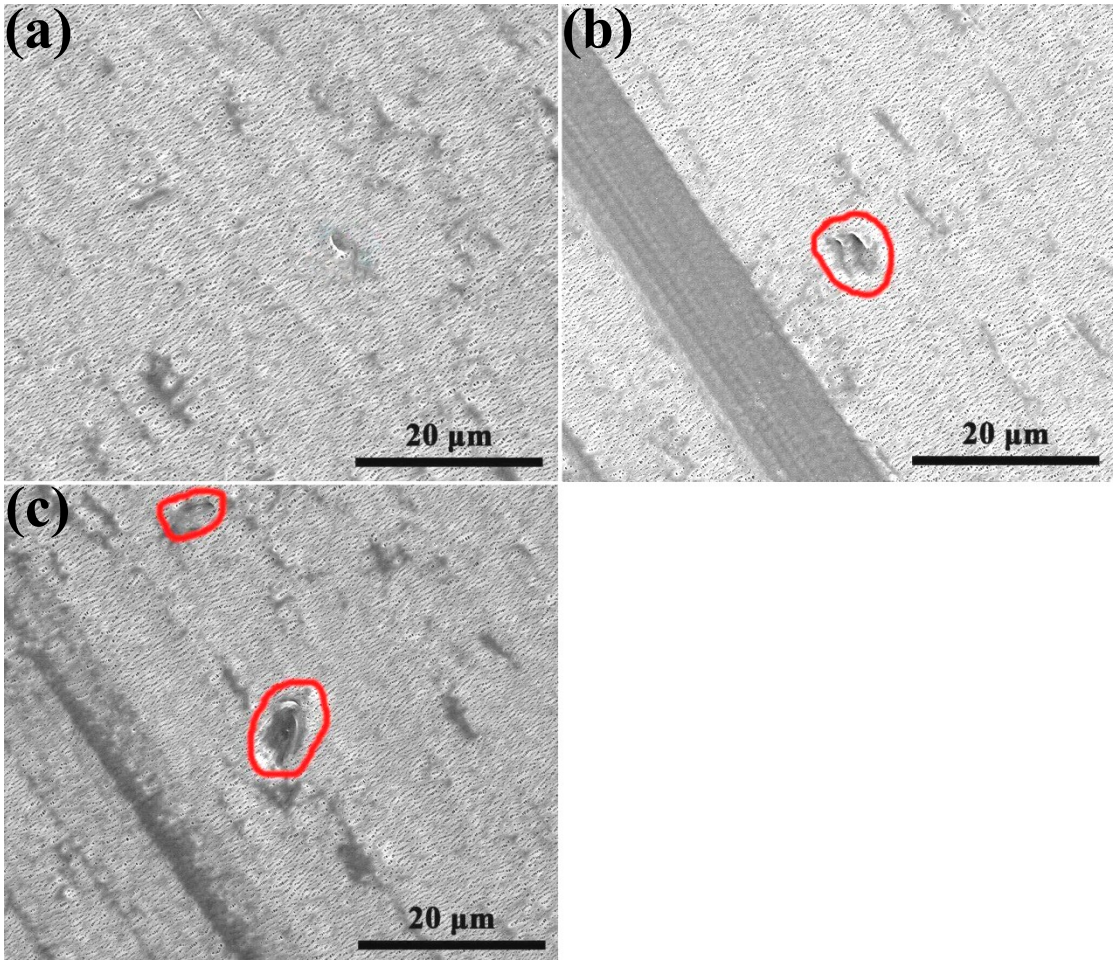

Figure S31 SEM images of the separator matched with PCNT-S@SNGE electrode cycled at rate of 15 C (a), 30 C (b), 40 C (c), respectively.

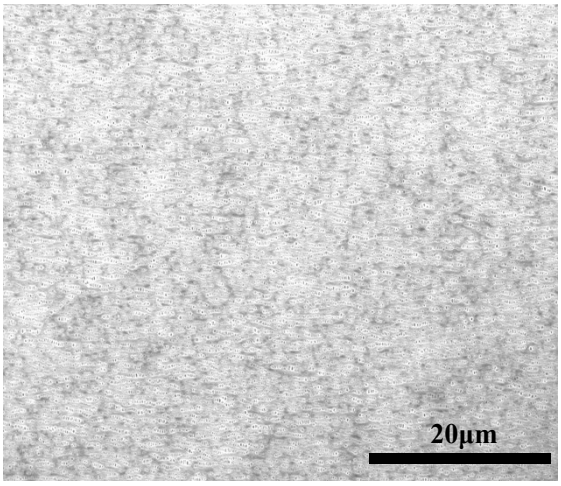

Figure S32 SEM image of the fresh separator.

References:

S1 K. Han, J. Shen, S. Hao, H. Ye, C. Wolverton, M. C. Kung, H. H. Kung, *Chem. Sus. Chem*. 2014, **7**, 2545-2553.